2-D Interference Channel Segmentation for Modified Factor Graph-Based Detection on BPMR System

Thanomsak Sopon[†], Non-member

ABSTRACT

In bit-patterned media recording (BPMR) systems can be increased to high areal density by reducing the size of the magnetic grains. When the magnetic grain sizes are smaller and closer, inter-track interference (ITI) problems occur. It is referred to as the two-dimensional (2-D) interference channel, which can degrade the read channel performance of the BPMR system. This article proposes two methods for an improved factor graph-based (FGB) detection using the 2-D interference channel coefficient segmentation that exploits the relationship between the main bit and its nearest neighbors. Both methods separate the 2-D interference channel into four clusters. Then, four clusters form a hierarchical message-passing relationship from the neighbor bits to the main bit. Simulation results show the bit error rate (BER) performance between the conventional FGB detector and the two methods of improved FGB detectors on the BPMR system at an areal density of 2.5 and 3 terabits per square inch (Tb/in^2) with multi-track processing. The BER performance of both modified FGB detectors outperforms the conventional FGB detector.

Keywords: Information storage, 2-D interference channel, factor graph-based detector, bit-patterned media recording

1. INTRODUCTION

Nowadays, the use of the internet is widespread, and there is a need to store a large amount of data, so the technology of hard disk drives has grown accordingly. A bit-patterned media recording (BPMR) system is one of the expectations for the next generation of magnetic recording technology to achieve an areal density of more than 1 terabit per square inch (Tb/in^2) [1]-[3]. As the areal density is increased the space between islands narrows. Thus, it produces the 2-D interference channel comprising inter-symbol interference (ISI) and inter-track interference (ITI) [4], [5]. That is one of the main limitations of the BPMR system because it reduces the efficiency of the BER in the read channel for the data recovery system. Moreover, it also creates a media noise, which is the fluctuation of magnetic grains in the along-track and across-track directions [6].

In recent years, researchers have worked on methods to correct defects in the 2-D interference channel and mitigate their effects using signal processing techniques for digital communication. Therefore, to resolve problems of the 2-D interference channel in the BPMR system, researchers have applied and developed signal processing approaches; for example, error control coding, modified equalizers and detectors, etc. The improved multi-track detection with a hybrid 2-D equalizer [7] appears as an alternative detector to reduce the 2-D interference channel. In [8], the parallel detection structure investigates the effect of the optimal weight of the average. As a result, the BER performance of the BPMR channel is significantly improved. However, from the point of view of multi-track signal processing and the joint detector algorithm subtracting the weighted summation is an alternative to use maximum-likelihood detection for the multi-head multi-track channels [9]. S. Han, *et al.* [10] proposed a detection scheme based on a multi-layer perceptron that estimates the track mis-registration and media noise. In particular, to minimize ISI and ITI, Y. Wang *et al.* [11] have proposed a recording scheme that uses multiple islands (2 by 2 islands) for one bit of information. In contrast, a traditional recording scheme records one bit on a single island. F. Ghanami *et al.* [12] presented a write channel model with input-dependent noise on a BPMR system by considering a binary random state, which obtains information rate lower and upper bounds and the gap. These lower and upper bounds are computed for the defined information rate in relation to the input distribution and first-order Markov process. S. Jeong *et al.* [13] proposed a bit-flipping scheme using the K-means algorithm, which is an iterative clustering method to identify samples consisting of the main and neighboring. Moreover, many researchers have introduced machine learning, deep learning and artificial neural networks, to reduce the problems of data detection and enable to increase the BER performance of magnetic recording systems [14]-[16].

This article has applied a factor graph-based (FGB) detector [17], [18] because it is a 2-D detector suitable for the BPMR system with multi-head multi-track processing. The FGB detector was developed from belief

Manuscript received on August 12, 2025; revised on October 22, 2025; accepted on December 4, 2025. This paper was recommended by Associate Editor Krit Angkeaw.

The author is with Department of Electronics Engineering, Rajamangala University of Technology Isan, Nakhon Ratchasima, Thailand.

[†]Corresponding author: thanomsak.so@rmuti.ac.th

Digital Object Identifier: 10.37936/ecti-eec.2026241.260631

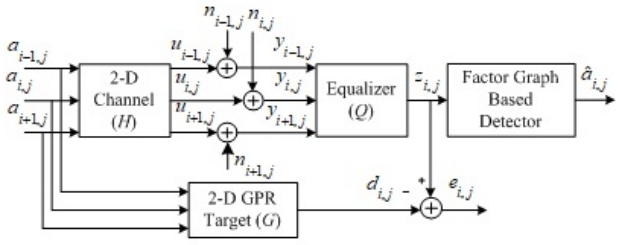

***Fig. 1**: Block diagram of read-write channel on BPMR system with multi-head multi-track processing.*

propagation algorithms. It works based on graphs that can use the information of neighbors to help design the processing, and to reduce the effect of the 2-D interference channel. Due to the increased areal density of the BPMR system, the impact of the 2-D interference channels will be also increased. Therefore, the improved FGB detector by separating the coefficients of the 2-D interference channel and performing hierarchical message-passing can increase the performance of the channel.

The rest of the paper is organized as follows. In Section II, we describe the introduction of the 2-D interference channel and equalizer model on the BPMR system. A modified factor graph-based detection is introduced in Section III. Section IV provides the simulation results and discussions. Finally, in Section V, we give the conclusion of the work.

2. BPMR CHANNEL AND EQUALIZER MODEL

A block diagram of the schematic of the read-write channel model is shown in Fig. 1. This system is similar to the conventional channel models, which show a BPMR channel model as the 2-D generalized partial response (GPR) target or 2-D interference channel, the equalizer and the FGB detector. We consider the read channel on a BPMR system with multi-track processing. In the read channel model $(a_{i,j}) = \{-1, 1\}$ is the recorded data bit on the j^{th} bit island along the i^{th} track, which generates the read-back signals $(y_{i,j})$ with additive white Gaussian noise (AWGN) $(n_{i,j})$ to be inputted to the equalizer $(z_{i,j})$ and then sent to the FGB detector so that the FGB detector can generate an estimated input bit $(\hat{a}_{i,j})$.

In this channel model, the 2-D interference channel response $h\ (m,\ n)$ is approximated by a 2-D Gaussian pulse response [6], which can be obtained as follows:

$$h(m,n) = \left(A + \Delta_A\right) \exp\left\{-\frac{1}{2c^2}\left[\left(\frac{T_x + \Delta_x}{PW_{50x}}\right)^2 + \left(\frac{T_z + \Delta_z}{PW_{50z}}\right)^2\right]\right\} \quad (1)$$

where $A = 1$ is the normalized peak amplitude of the pulse response. Δ_A is the amplitude fluctuation. T_x is the bit period, T_z is the track pitch, Δ_x is the fluctuation in along-track, and Δ_z is the fluctuation in across-track; x and z are indices in along-track and across-track directions,

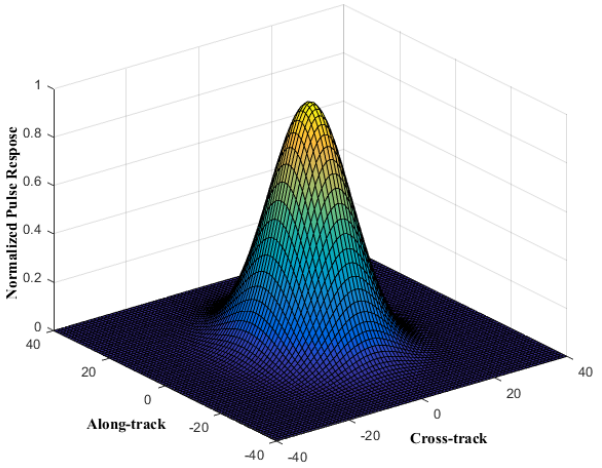

***Fig. 2**: Numerical 2-D Gaussian pulse response of the square island.*

respectively. PW_{50x} and PW_{50z} are the widths of the pulse response at its half maximum in along-track and across-track directions, respectively. c is a constant to account for the relationship between 50% pulse width and the standard deviation of the Gaussian function.

For the pulse model in Equation (1), the parameters related to the 2-D Gaussian pulse response are given as follows: $A = 1$, $PW_{50z} = 24.8$ nm, $PW_{50x} = 19.4$ nm, and $c = 1/2.3548$. The simulated 2-D Gaussian pulse response of an isolated square island with a length of 14.5 nm, as shown in Fig. 2.

The discrete-time read-back signal is determined by the position of the data bit. If parameters i and j denote the island position in across-track and along-track directions, respectively. The coefficients of the 2-D interference channel response $(h_{i,j})$ are a convolution operator on the bit input signal and combined with AWGN to obtain the read-back signal $(y_{i,j})$, which can be written as

$$y_{i,j} = \left(a_{i,j} \otimes h_{i,j}\right) + n_{i,j}. \quad (2)$$

That, can be expressed as

$$y_{i,j} = \sum_{m=-M}^{M} \sum_{n=-N}^{N} a_{i-m,j-nh_{m,n}} + n_{i,j}. \quad (3)$$

where $h_{m,n}$ is the coefficient of the discrete-time 2-D interference channel, which is obtained by sampling the pulse signal at times that are multiples of the bit time and track period. M and N are the lengths of the interference from neighboring islands in the along-track and across-track directions. We set $M = 1$ and $N = 1$. Hence, a 2-D interference channel matrix H is given by

$$\mathbf{H} = \begin{bmatrix} h_{-1,-1} & h_{-1,0} & h_{-1,1} \\ h_{0,-1} & h_{0,0} & h_{0,1} \\ h_{1,-1} & h_{1,0} & h_{1,1} \end{bmatrix}. \quad (4)$$

Since a 2-D interference channel can be written in matrix **H** from Equation (4). Then the read-back signal in Equation (3) can be expanded as

$$\begin{aligned} y_{i,j} &= a_{i-1,j-1}h_{-1,-1} + a_{i,j-1}h_{0,-1} + a_{i+1,j-1}h_{1,-1} \\ &\quad + a_{i-1,j}h_{-1,0} + a_{i,j}h_{0,0} + a_{i+1,j}h_{1,0} \\ &\quad + a_{i-1,j+1}h_{-1,1} + a_{i,j+1}h_{0,1} + a_{i+1,j+1}h_{1,1} + n_{i,j} \end{aligned} \quad (5)$$

Afterward, the 2-D GPR target and the 2-D equalizer are designed based on the minimum mean squared error (MMSE) technique [19]-[20]. We consider the BPMR system, which recovers the recorded data ($a_{i,j}$) from the main track i = 0. Let the 2-D GPR target (**G**) be represented as a 3×3 matrix, and an equalizer (**Q**) matrix with a size of 3×7 can be represented by the following matrix:

$$\mathbf{G} = \begin{bmatrix} g_{i-1,j-1} & g_{i-1,j} & g_{i-1,j+1} \\ g_{i,j-1} & g_{i,j} & g_{i,j+1} \\ g_{i+1,j-1} & g_{i+1,j} & g_{i+1,j+1} \end{bmatrix}, \quad (6)$$

and

$$\mathbf{Q} = \begin{bmatrix} q_{i-1,j-3} & \cdots & q_{i-1,j} & \cdots & q_{i-1,j+3} \\ q_{i,j-3} & \cdots & q_{i,j} & \cdots & q_{i,j+3} \\ q_{i+1,j-3} & \cdots & q_{i+1,j} & \cdots & q_{i+1,j+3} \end{bmatrix}. \quad (7)$$

For the input of an equalization, the adjacent read-back signals ($r_{i,j}$) are required to produce a single output ($z_{i,j}$), because it includes the contribution of the adjacent tracks.

$$z_{i,j} = \mathbf{q}^T\mathbf{r} \quad (8)$$

$$d_{i,j} = \mathbf{g}^T\mathbf{a} \quad (9)$$

Since the input bit sequences ($a_{i,j}$) are fed to a 2-D GPR target to obtain the desired output ($d_{i,j}$). To calculate the coefficients of the equalizer and the 2-D target polynomial, we define the error signal ($e_{i,j}$) as follows:

$$e_{i,j} = z_{i,j} - d_{i,j}. \quad (10)$$

Here,

$$\mathbf{q} = \begin{bmatrix} q_{i-1,j-3} & q_{i-1,j-2} & \dots & q_{i,j} & \dots & q_{i+1,j+2} & qi_{+1,j+3} \end{bmatrix}^T$$

$$\mathbf{g} = \begin{bmatrix} g_{i-1,j-1} & g_{i-1,j} & \dots & g_{i,j} & \dots & g_{i+1,j} & g_{i+1,j+1} \end{bmatrix}^T$$

$$\mathbf{r} = \begin{bmatrix} r_{i+3,j+3} & r_{i+3,j+2} & \dots & r_{i,j} & \dots & r_{i-3,j-2} & r_{i-3,j-3} \end{bmatrix}^T$$

$$\mathbf{a} = \begin{bmatrix} a_{i+1,j+1} & a_{i+1,j} & \dots & a_{i,j} & \dots & a_{i-1,j} & a_{i-1,j-1} \end{bmatrix}^T$$

Next, we can calculate the error signal ($e_{i,j}$) by the MSE, which is calculated as

$$\begin{aligned} E\left\{(e_{i,j})^2\right\} &= E\left\{\left(\mathbf{q}^T\mathbf{r}-\mathbf{g}^T\mathbf{a}\right)\left(\mathbf{q}^T\mathbf{r}-\mathbf{g}^T\mathbf{a}\right)\right\} \\ &= \mathbf{q}^T\mathbf{R}\mathbf{q} - 2\mathbf{q}^T\mathbf{T}\mathbf{g} + \mathbf{g}^T\mathbf{A}\mathbf{g} \end{aligned} \quad (11)$$

Therefore, the constraint can be expressed as follows

$$\mathbf{E}^{\mathrm{T}}\mathrm{g} = \mathrm{I} \quad (12)$$

where

$$\mathbf{I} = \begin{bmatrix} 1 & 0 & 0 & 0 & 0 & 0 & 0 \end{bmatrix}^T, \quad (13)$$

and

$$\mathbf{E}^T = \begin{bmatrix} 0 & 0 & 0 & 0 & 1 & 0 & 0 & 0 & 0 \\ 1 & 0 & 0 & 0 & 0 & 0 & 0 & 0 & 0 \\ 0 & 1 & 0 & 0 & 0 & 0 & 0 & 0 & 0 \\ 0 & 0 & 1 & 0 & 0 & 0 & 0 & 0 & 0 \\ 0 & 0 & 0 & 0 & 0 & 0 & 1 & 0 & 0 \\ 0 & 0 & 0 & 0 & 0 & 0 & 0 & 1 & 0 \\ 0 & 0 & 0 & 0 & 0 & 0 & 0 & 0 & 1 \end{bmatrix} \quad (14)$$

Based on this monic constraint, the optimized target and equalizer coefficient vector can be derived as

$$\lambda = \left(\mathbf{E}^{\mathrm{T}}\left(\mathrm{A} - \mathrm{T}^{\mathrm{T}}\mathrm{R}^{-1}\mathrm{T}\right)^{-1}\mathrm{E}\right)^{-1}\mathrm{I} \quad (15)$$

$$\mathbf{g} = \left(\mathbf{A} - \mathbf{T}^T\mathbf{R}^{-1}\mathbf{T}\right)^{-1}\mathbf{E}\lambda \quad (16)$$

$$\mathbf{q} = \mathbf{R}^{-1}\mathbf{T}\mathbf{g} \quad (17)$$

where, λ is a vector containing the Lagrange multipliers. **g** and **q** are the optimized target and equalizer coefficients.

Hence, $\mathbf{A} = E\left\{\mathbf{a}_i, \mathbf{a}_i^T\right\}$is the autocorrelation of the input. $\mathbf{R} = E\left\{\mathbf{r}_i, \mathbf{r}_i^T\right\}$ is the autocorrelation matrix of the channel output. $\mathbf{T} = E\left\{\mathbf{r}_i, \mathbf{a}_i^T\right\}$ is the cross-correlation of the channel output and input, where E denotes the expectation operator.

3. FACTOR GRAPH-BASED DETECTION

In this section, a factor graph-based (FGB) detection is performed by using the factor graph to process the received signal from the 2-D interference channel, as shown in Fig. 1. Since the FGB detector is designed based on the 2-D interference channel using *a posteriori* log-likelihood ratio (LLR) as the message-passing [17], [18]. The 2-D interference channel with a 3 by 3 matrix is converted into a 1-D array with a 1 by 9 matrix, which consists of the factor node and bit node. The factor node represents the read-back signals, and the bit node represents the bit inputs. An edge between the factor node and the bit node is the LLR reliability information that is based on the received signal. During the iterative processing, the factor node and the bit node exchange the reliability information.

In Fig. 3, the factor node $\{y_{i,j}\}$ (solid line) passes the reliability information to the connected nine bit nodes as $\{a_{i-1,j-1}, a_{i-1,j}, a_{i-1,j+1}, a_{i,j-1}, a_{i,j}, a_{i,j+1}, a_{i+1,j-1}, a_{i+1,j}, a_{i+1,j+1}\}$. Then, at each bit node $\{a_{i-1,j-1}, a_{i-1,j}, a_{i-1,j+1}, a_{i,j-1}, a_{i,j}, a_{i,j+1}, a_{i+1,j-1}, a_{i+1,j}, a_{i+1,j+1}\}$ updates and sends back the information to the connected eight factor nodes (dashed line) $\{y_{i-1,j-1}, y_{i-1,j}, y_{i-1,j+1}, y_{i,j-1}, y_{i,j+1}, y_{i+1,j-1}, y_{i+1,j}, y_{i+1,j+1}\}$, except for the factor node $\{y_{i,j}\}$. Before sending the message, each

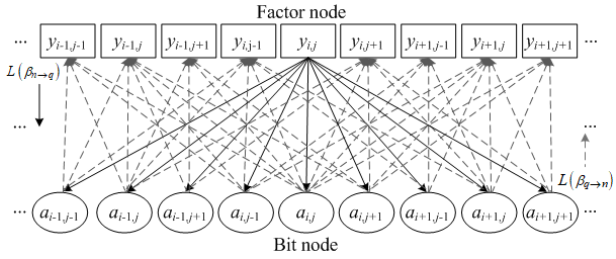

***Fig. 3**: Scheme of factor graph of 2-D interference channel.*

factor node computes the reliability information based on the read-back signal.

The message-passing algorithm is the log-maximum *a posteriori* probability (MAP) algorithm [21], which calculates the LLR reliability information between the factor nodes and the bit nodes on a factor graph, as follows:

$$L\left(\beta_{n\to q}\right)=\log\frac{\Pr\left(a_n=+1\mid u_n\right)}{\Pr\left(a_n=-1\mid u_n\right)}$$

$$=\log\frac{\sum_{\Delta^n;a_q=+1}\Pr\left(u_n\mid\Delta^n_{\sim a_q},a_k=+1\right)\Pr\left(\Delta^n_{\sim a_q}\right)}{\sum_{\Delta^n;a_q=+1}\Pr\left(u_n\mid\Delta^n_{\sim a_q},a_k=-1\right)\Pr\left(\Delta^n_{\sim a_q}\right)}. \tag{18}$$

where u_n is the received signal without noise, y_n is the read-back signal with AWGN noise, and σ^2 is the variance of AWGN.

We consider the log-MAP algorithm to compute the reliability information from Equation (18). Accordingly, the messages $L(\mu_{k\to n})$ are generated from connected the bit node k to the factor node n, which can be rewritten as

$$L\left(\mu_{n\to q}\right)=\log\frac{\sum_{\Delta^n;a_q=+1}\exp\left(-\frac{\left(y_n-u_n\right)^2}{2\sigma^2}+\sum_{k\in\Delta^n_{\sim a_q},a_k=+1}L(\mu_{k\to n})\right)}{\sum_{\Delta^n;a_q=-1}\exp\left(-\frac{\left(y_n-u_n\right)^2}{2\sigma^2}+\sum_{k\in\Delta^n_{\sim a_q},a_k=-1}L(\mu_{k\to n})\right)} \tag{19}$$

In the reverse direction, each bit node receives the LLR message from the factor nodes. After that, the LLR message is sent from bit nodes q to the factor nodes n, which is computed as

$$L\left(\mu_{q\to n}\right)=\sum_{r\in B_n^q}L\left(\mu_{r\to q}\right) \tag{20}$$

where B_n^q is the number of factor nodes that are connected to the bit nodes.

These updating and exchanging reliability information processes will continue until a final iteration is reached. After several predetermined iterations $L\left(\hat{a}_n\right)$, the final soft output of summation is given by

$$L\left(\hat{a}_n\right)=\sum L\left(\mu_{k\to n}\right). \tag{21}$$

In the final step, a hard estimation of the input bit is defined as

$$\hat{a}_n=\begin{cases}+1, & \text{if } L\left(\hat{a}_n\right)\geq 0\\ -1, & \text{otherwise}\end{cases} \tag{22}$$

In this research, we propose two methods for the 2-D interference channel segmentation, which separate the coefficients of the 2-D interference channel into four cluster channels. By taking advantage of hierarchical message-passing on the factor graph between the factor node and the bit node. The factor graph design is based on four cluster channels of the 2-D interference channel segmentation.

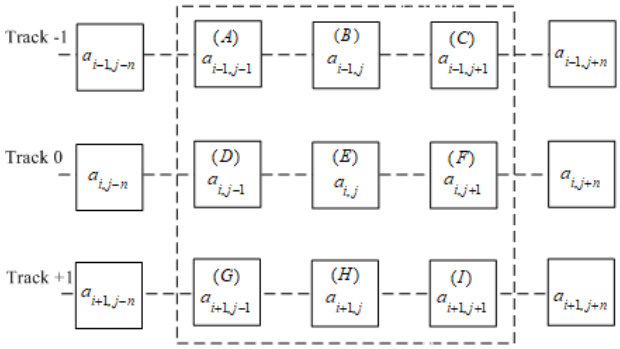

***Fig. 4**: Scheme of square array islands between main and neighboring islands.*

Figure 4 shows the configuration of the patterned islands for the coefficients of a 2-D interference channel with a 3 by 3 matrix (dashed square) in Equation (4), as follows: $\{A=h_{i-1,j-1}, B=h_{i-1,j}, C=h_{i-1,j+1}, D=h_{i,j-1}, E=h_{i,j}, F=h_{i,j+1}, G=h_{i+1,j-1}, H=h_{i+1,j}, I=h_{i+1,j+1}\}$. Therefore, the improvements of the two FGB detectors can be presented as follows.

3.1 Modified FGB Detector (M1)

In relation-structure, we apply a generalized belief propagation (GBP) algorithm [22] to the FGB detector. A factor graph designs the coefficients of the 2-D interference channel, which are arranged in a one-dimensional (1-D) array based on the relationship between the main bit E and the neighboring data bits A, B, C, D, F, G, H, and I. Figure 5 shows the structure of hierarchical message-passing on a factor graph, in which the 2-D interference channel can be separated into four clusters of six nodes: $\{A, B, C, D, E, F\}$, $\{D, E, F, G, H, I\}$, $\{A, B, D, E, G, H\}$ and $\{B, C, E, F, H, I\}$. All four clusters send LLR belief propagations to calculate the relationship of the nodes $\{B, E\}$, $\{D, E\}$, $\{F, E\}$ and $\{H, E\}$. Next, they calculate the main bit $\{E\}$.

In the first step, we can consider the message-passing structure of the four cluster channels: $\{A, B, C, D, E, F\}$,

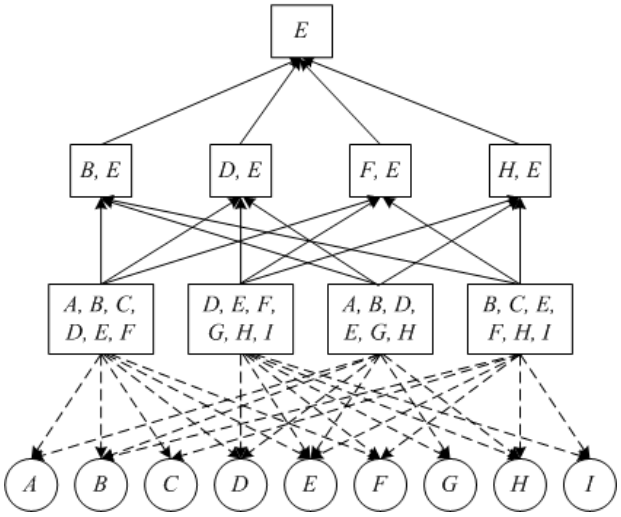

***Fig. 5**: Structure of hierarchical message-passing of factor graph on 2-D interference channel for modified FGB detector (M1).*

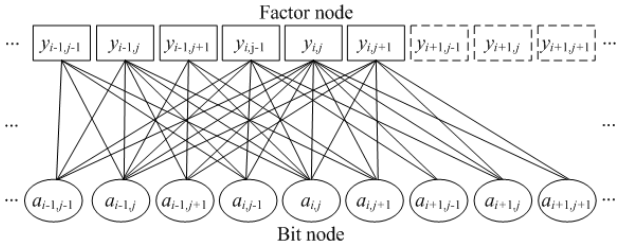

***Fig. 6**: A factor graph represents the message-passing of {A, B, C, D, E, F} channel.*

{*D, E, F, G, H, I*}, {*A, B, D, E, G, H*} and {*B, C, E, F, H, I*}, which are the message-passing of the LLR reliability information from the factor node to the bit nodes (*A*), (*B*), (*C*), (*D*), (*E*), (*F*), (*G*), (*H*), and (*I*). Each channel of the factor graph calculates the LLR reliability information between the factor node and the bit node according to Equation (19) and Equation (20), and all four clusters represent the factor graph relationship as follows.

In Fig. 6, a factor graph represents the message-passing of {*A, B, C, D, E, F*} channel. The factor node $\{y_{i-1,j-1}, y_{i-1,j}, y_{i-1,j+1}, y_{i,j-1}, y_{i,j}, y_{i,j+1}\}$ passes the reliability information to the connected bit nodes $\{a_{i-1,j-1}, a_{i-1,j}, a_{i-1,j+1}, a_{i,j-1}, a_{i,j}, a_{i,j+1}, a_{i+1,\,j-1}, a_{i+1,j}, a_{i+1,j+1}\}$. After that, the bit nodes $\{a_{i-1,j-1}, a_{i-1,j}, a_{i-1,j+1}, a_{i,j-1}, a_{i,j}, a_{i,j+1}, a_{i+1,j-1}, a_{i+1,j}, a_{i+1,j+1}\}$ are updated with the reliability information and sent to their corresponding factor nodes.

In the same way, a factor graph of {*D, E, F, G, H, I*} channel, the factor node $\{y_{i,j-1}, y_{i,j}, y_{i,j+1}, y_{i+1,j-1}, y_{i+1,j}, y_{i+1,j+1}\}$ send the reliability information to connect the bit nodes $\{a_{i-1,j-1}, a_{i-1,j}, a_{i-1,j+1}, a_{i,j-1}, a_{i,j}, a_{i,j+1}, a_{i+1,j-1}, a_{i+1,j}, a_{i+1,j+1}\}$. Next, each bit node sends back the connected respective factor nodes, as shown in Fig. 7.

Figure 8 shows the factor graph of {*A, B, D, E, G, H*} channel. Factor node $\{y_{i-1,j-1}, y_{i-1,j}, y_{i,j-1}, y_{i,j}, y_{i+1,j-1}, y_{i+1,j}\}$ passes the reliability information to connect bit nodes $\{a_{i-1,j-1}, a_{i-1,j}, a_{i-1,j+1}, a_{i,j-1}, a_{i,j}, a_{i,j+1}, a_{i+1,j-1}, a_{i+1,j}, a_{i+1,j+1}\}$, then each bit node sends to the connected factor nodes. ***Fig. 8:** A factor graph represents the message-passing of {A, B, D, E, G, H} channel.*

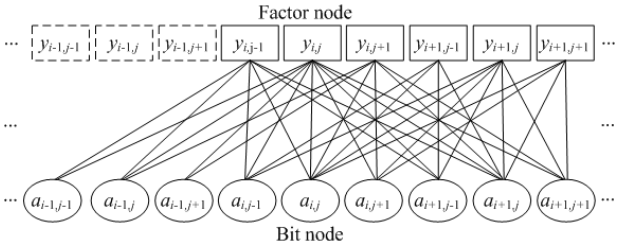

***Fig. 7**: A factor graph represents the message-passing of {D, E, F, G, H, I} channel.*

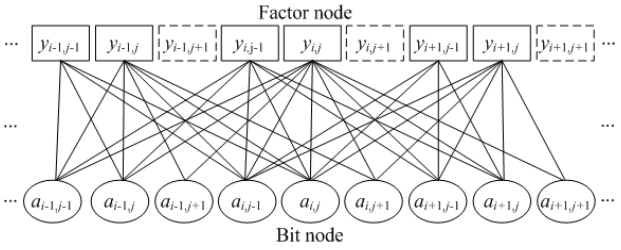

***Fig. 8**: A factor graph represents the message-passing of {A, B, D, E, G, H} channel.*

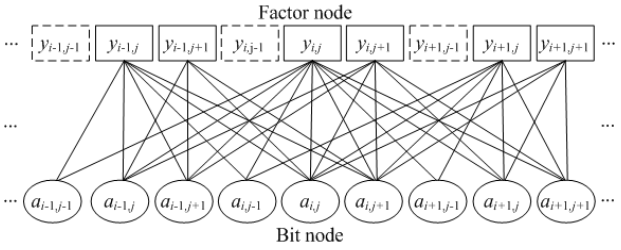

***Fig. 9**: A factor graph represents the message-passing of {B, C, E, F, H, I} channel.*

A factor graph of {*B, C, E, F, H, I*} channel, factor node $\{y_{i-1,j}, y_{i-1,j+1}, y_{i,j}, y_{i,j+1}, y_{i+1,j}, y_{i+1,j+1}\}$ send the reliability information to connect bit nodes $\{a_{i-1,j-1}, a_{i-1,j}, a_{i-1,j+1}, a_{i,j-1}, a_{i,j}, a_{i,j+1}, a_{i+1,j-1}, a_{i+1,j}, a_{i+1,j+1}\}$, therefrom each bit node sends back the connected respective factor nodes, as shown in Fig. 9.

When the LLR reliability information is received from the four cluster channels; {*A, B, C, D, E, F*}, {*D, E, F, G, H, I*}, {*A, B, D, E, G, H*} and {*B, C, E, F, H, I*}. In the second step, we represent the message-passing relationship based on the hierarchical structure between the channels of the four clusters. In Fig. 10, the message is the LLR reliability information passing along the edge between the nodes. The message is only based on the influence of a node and its adjacent neighbor. For example, in Figure 10 (*a*) shows the {*A, B, C, D, E, F*}

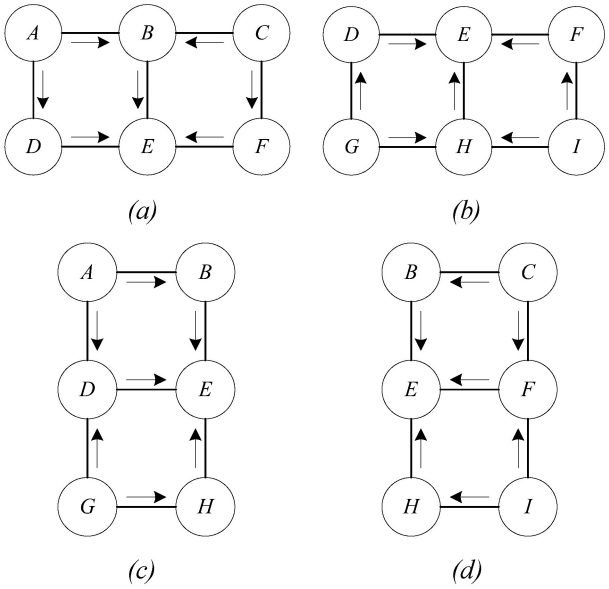

***Fig. 10**: A region graph generated using the cluster method for message-passing of the channels; (a) {A, B, C, D, E, F}, (b) {D, E, F, G, H, I}, (c) {A, B, D, E, G, H}, and (d) {B, C, E, F, H, I}*

channel, in which the main bit $\{E\}$ is received by the message from the neighboring nodes, namely: $\{A, B\}$, $\{B, E\}$, $\{A, D\}$, $\{D, E\}$, $\{C, B\}$, $\{C, F\}$ and $\{F, E\}$. Similarly, $\{D, E, F, G, H, I\}$ channel is the message-passing from relationship nodes $\{G, D\}$, $\{D, E\}$, $\{G, H\}$, $\{H, E\}$, $\{I, F\}$, $\{F, E\}$ and $\{I, H\}$, $\{A, B, D, E, G, H\}$ channel is the nodes relationship $\{A, B\}$, $\{B, E\}$, $\{A, D\}$, $\{D, E\}$, $\{G, D\}$, $\{G, H\}$ and $\{H, E\}$, $\{B, C, E, F, H, I\}$ channel is the nodes relationship $\{C, B\}$, $\{B, E\}$, $\{C, F\}$, $\{F, E\}$, $\{I, F\}$, $\{I, H\}$ and $\{H, E\}$ to determine the main bit $\{E\}$, as shown in Fig. 10 (*b*), (*c*) and (*d*), respectively.

After that, an approximation of the relationship among $\{A, B, C, D, E, F\}$, $\{D, E, F, G, H, I\}$, $\{A, B, D, E, G, H\}$, and $\{B, C, E, F, H, I\}$ channels can be written as

$$H_{ABCDEF} = H_{AB} + H_{BE} + H_{AD} + H_{DE} + H_{CB} + H_{CF} + H_{FE} - H_A - H_B - H_C - H_D - H_E - H_F, \quad (23)$$

$$H_{DEFGHI} = H_{GD} + H_{DE} + H_{GH} + H_{HE} + H_{IF} + H_{FE} + H_{IH} - H_D - H_E - H_F - H_G - H_H - H_I, \quad (24)$$

$$H_{ABDEGH} = H_{AB} + H_{BE} + H_{AD} + H_{DE} + H_{GD} + H_{GH} + H_{HE} - H_A - H_B - H_D - H_E - H_G - H_H, \quad (25)$$

$$H_{BCEFHI} = H_{CB} + H_{BE} + H_{CF} + H_{FE} + H_{IF} + H_{IH} + H_{HE} - H_B - H_C - H_E - H_F - H_H - H_I. \quad (26)$$

Next, estimating the summation in Equation (23) to Equation (26), the $H_{(M1)}$ channel can be obtained from

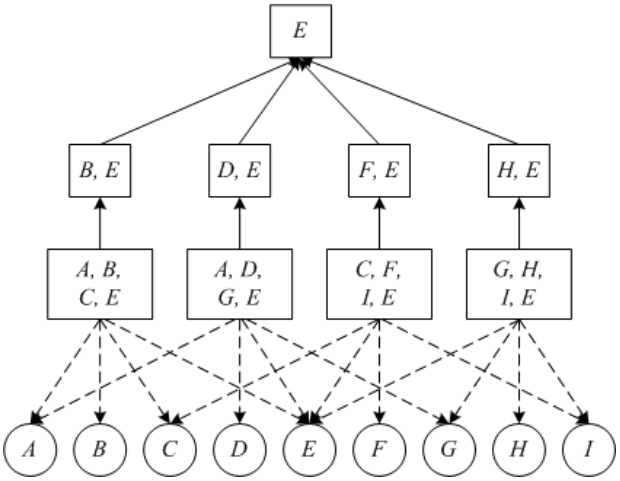

***Fig. 11**: Scheme of hierarchical message-passing of factor graph on 2-D interference channel for modified FGB detector (M2).*

$$H_{(M1)} = H_{ABCDEF} + H_{DEFGHI} + H_{ABDEGH} + H_{BCEFHI} - H_{BE} - H_{DE} - H_{EF} - H_{EH} + H_E. \quad (27)$$

From Equation (27), the final result of the combination is calculated from Equation (21) and the input estimation according to Equation (22).

3.2 Modified FGB Detector (M2)

In this second method, we separate the coefficients of the 2-D interference channel into four clusters, each cluster containing four nodes, namely $\{A, B, C, E\}$, $\{A, D, G, E\}$, $\{C, F, I, E\}$ and $\{G, H, I, E\}$. The message-passing is similar to the first method; the messages are sent on the factor graph with a hierarchical message-passing structure, which can be clustered into four channels of four-node clusters, $\{A, B, C, E\}$, $\{A, D, G, E\}$, $\{C, F, I, E\}$ and $\{G, H, I, E\}$ based on the relationship among the main data bit (E) and its neighboring data bits (A), (B), (C), (D), (F), (G), (H), and (I). Next, to receive the LLR belief propagation for determining the relation of $\{B, E\}$, $\{D, E\}$, $\{F, E\}$ and $\{H, E\}$. The message-passing computes the main bit $\{E\}$, as shown in Fig. 11.

After separating 2-D interference channel coefficients into four cluster channels $\{A, B, C, E\}$, $\{A, D, G, E\}$, $\{C, F, I, E\}$ and $\{G, H, I, E\}$, each channel of the factor graph computes the LLR reliability information between the factor node and the bit node according to Equation (19) and Equation (20). The factor graph is the relationship of $\{A, B, C, E\}$ channel with the factor node $\{y_{i-1,j-1}, y_{i-1,j}, y_{i-1,j+1}, y_{i,j}\}$, $\{A, D, G, E\}$ channel with the factor node $\{y_{i-1,j-1}, y_{i,j-1}, y_{i+1,j-1}, y_{i,j}\}$, $\{C, F, I, E\}$ channel with the factor node $\{y_{i-1,j+1}, y_{i,j+1}, y_{i+1,j+1}, y_{i,j}\}$, and $\{G, H, I, E\}$ channel with the factor node $\{y_{i+1,j-1}, y_{i+1,j}, y_{i+1,j+1}, y_{i,j}\}$, respectively. The factor nodes of

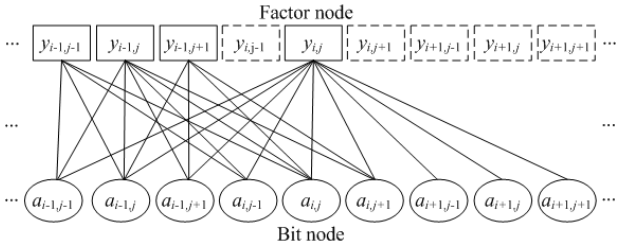

***Fig. 12**: A factor graph represents the message-passing of {A, B, C, E} channel.*

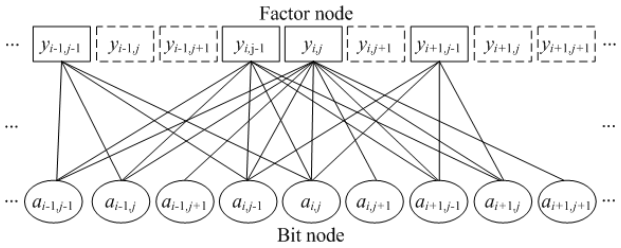

***Fig. 13**: A factor graph represents the message-passing of {A, D, G, E} channel.*

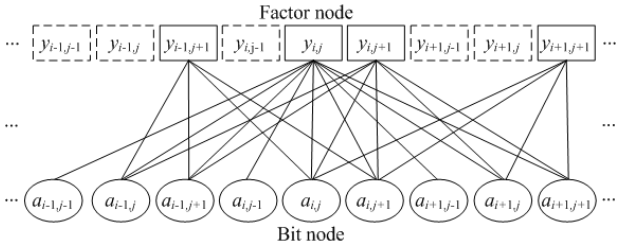

***Fig. 14**: A factor graph represents the message-passing of {C, F, I, E} channel.*

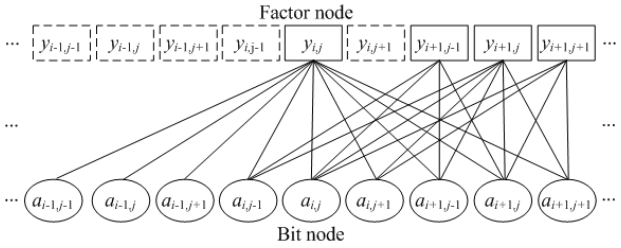

***Fig. 15**: A factor graph represents the message-passing of {G, H, I, E} channel.*

the four cluster channels pass the reliability information to the connected bit nodes $\{a_{i-1,j-1},\ a_{i-1,j},\ a_{i-1,j+1},\ a_{i,j-1},\ a_{i,j},\ a_{i,j+1},\ a_{i+1,j-1},\ a_{i+1,j},\ a_{i+1,j+1}\}$. Then the bit nodes $\{a_{i-1,j-1},\ a_{i-1,j},\ a_{i-1,j+1},\ a_{i,j-1},\ a_{i,j},\ a_{i,j+1},\ a_{i+1,j-1},\ a_{i+1,j},\ a_{i+1,j+1}\}$ are updated and sent to the corresponding factor nodes according to the relationship of each channel, as shown in Fig. 12 to Fig. 15, respectively.

In the next step, the LLR reliability information is received from the four clusters, and then the related message-passing channels are considered hierarchically

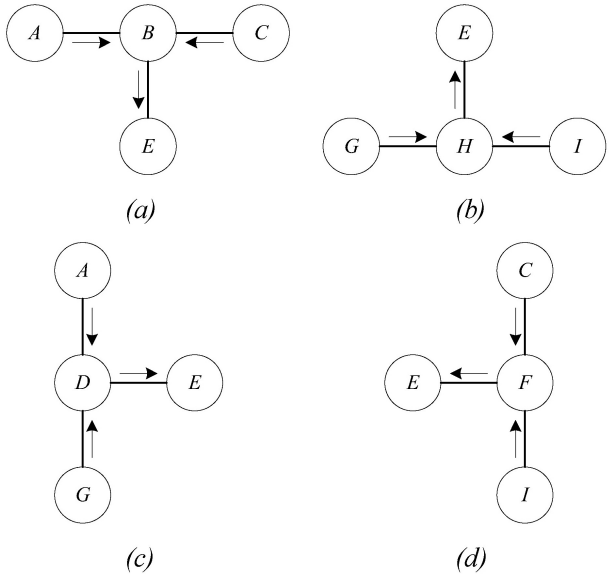

***Fig. 16**: A region graph generated using the cluster method for message-passing of the channels; (a) {A, B, C, E}, (b) {G, H, I, E}, (c) {A, D, G, E}, and (d) {C, F, I, E}.*

as the first method. The main bit {*E*} of {*A, B, C, E*}, {A, *D, G, E*}, {*C, F, I, E*} and {*G, H, I, E*} channels are received by the messages of the correlations from neighboring nodes, namely: {*B, E*}, {*D, E*}, {*F, E*} and {*H, E*}, as shown in Fig. 16 (*a*), (*b*), (*c*) and (*d*), respectively.

To estimate the relationship among {*A, B, C, E*}, {*G, H, I, E*}, {*A, D, G, E*}, and {*C, F, I, E*} channels, which is given by

$$H_{ABCE} = H_{AB} + H_{CB} + H_{BE} - H_A - H_B - H_C - H_E, \quad (28)$$

$$H_{GHIE} = H_{GH} + H_{IH} + H_{HE} - H_G - H_H - H_I - H_E, \quad (29)$$

$$H_{ADGE} = H_{AD} + H_{GD} + H_{DE} - H_A - H_D - H_G - H_E, \quad (30)$$

$$H_{CFIE} = H_{CF} + H_{IF} + H_{FE} - H_C - H_F - H_I - H_E. \quad (31)$$

Therefore, from Equation (28) to Equation (31), the relationship of the $H_{(M2)}$ channel can be written as follows

$$H_{(M2)} = H_{ABCE} + H_{ADGE} + H_{CFIE} + H_{GHIE} - H_{BE} - H_{DE} - H_{FE} - H_{HE} + H_E \quad (32)$$

In Equation (32), the final result of the combination and the input estimation are calculated from Equation (21) and Equation (22), respectively.

4. SIMULATION AND RESULTS

In this section, we consider the BPMR channel at an areal density of 2.5 and 3 Tb/in^2 with multi-track processing, in which both bit period and track pitch are 16 nm and 14.5 nm, respectively. The along-track PW_{50x} is 19.4 nm, and the across-track PW_{50z} is 24.8 nm. For the system, each sector includes 4,096 bits. From

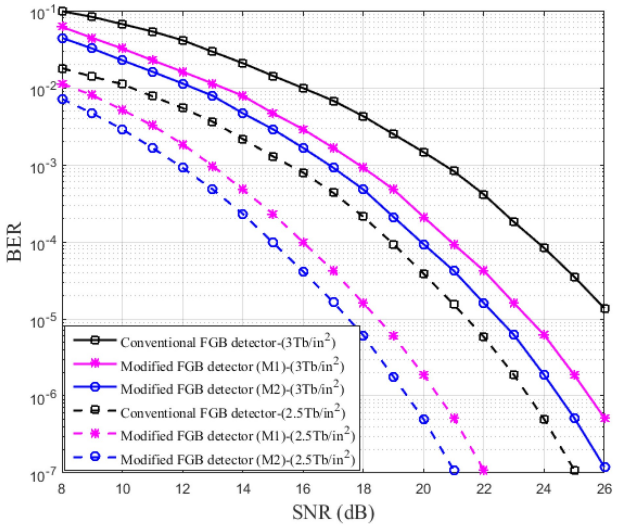

***Fig. 17**: BER performance Comparison of conventional FGB detector and modified FGB detectors on BPMR channel at areal density of 2.5 and 3 Tb/in^2.*

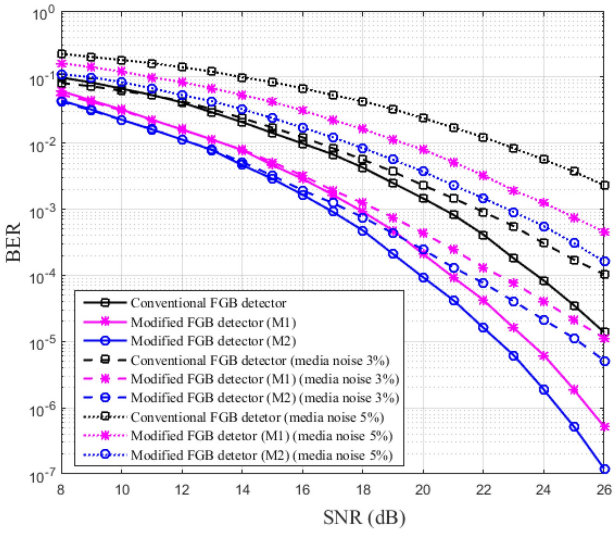

***Fig. 18**: BER performance comparison between the conventional FGB detector and modified FGB detectors on BPMR channel at areal density of 3 Tb/in^2 with media noise.*

Equation (4), the 3×3 matrix of a 2-D interference channel is generated by a 2-D Gaussian function from Equation (1) as

$$\mathbf{H}(2.5Tb) = \begin{bmatrix} 0.0478 & 0.3154 & 0.0478 \\ 0.1517 & 1.0000 & 0.1517 \\ 0.0478 & 0.3154 & 0.0478 \end{bmatrix},$$

and

$$\mathbf{H}(3Tb) = \begin{bmatrix} 0.0824 & 0.3876 & 0.0824 \\ 0.2125 & 1.0000 & 0.2125 \\ 0.0824 & 0.3876 & 0.0824 \end{bmatrix}.$$

In the following analysis, the signal-to-noise ratio (SNR) is defined as

$$SNR\,(\mathrm{dB}) = 10\log_{10}\frac{V_p}{\sigma^2}. \tag{33}$$

where $V_p = 1$ is the normalized peak value of the read-back signal and σ is the standard deviation of the AWGN.

Figure 17 shows the BER performance between the conventional FGB detector and modified FGB detectors (M1) and (M2) in the BPMR channel at an areal density of 2.5 Tb/in^2 without media noise. The modified FGB detector (M1) achieves gains of about 3.0 dB over the conventional FGB detector at BER equal to 10^{-6}. The performance comparison of the modified FGB detector (M2) is better than the modified FGB detector (M1) in SNR of 1.0 dB at BER equal to 10^{-6}. Moreover, the modified FGB detectors (M1) and (M2) are better than the conventional FGB detector on the BPMR channel at an areal density of 3 Tb/in^2.

In the simulation, the BPMR channel at an areal density of 3 Tb/in^2 with media noise indicates the effect of the size and position fluctuations of the islands in along-track and across-track directions. In Fig. 18, we evaluate the BER performance of the conventional FGB detector, modified FGB detector (M1) and modified FGB detector (M2). When the media noise level increases by 3% and 5%, it will decrease the BER performance significantly.

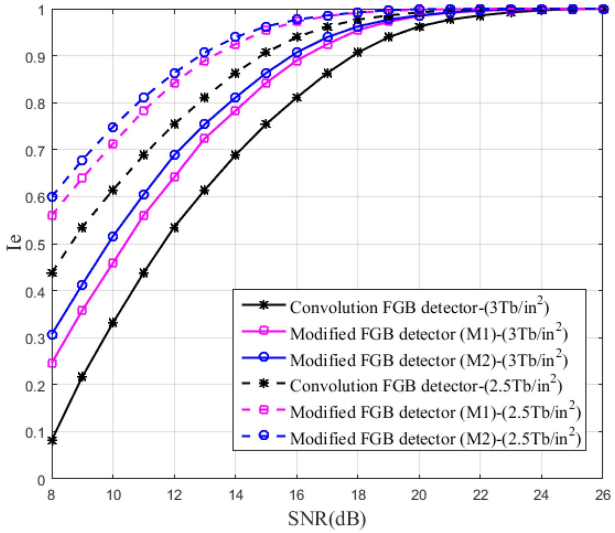

***Fig. 19**: Comparison of performance based on mutual information for conventional FGB detector, modified FGB detector (M1) and modified FGB detector (M2).*

Additionally, we have measured the outputs of mutual information [23] to compare the performance of the three detectors. The mutual information $M(C;A)$ between a bit of a random variable A and its LLR information of each bit consistent C-value is defined as

$$M(C;A) = 1 - \int_{-\infty}^{+\infty} \rho(C|a=+1)\log_2\left(1+\exp^{-C}\right) dC \tag{34}$$

***Table 1**: Complexity Computation of Detectors.*

Detectors	Complexity O(.)	$I = 3$
Conventional FGB detector	$I \times L(2^9) = 512IL$	$1{,}536L$
Modified FGB detector (M1)	$I \times L(2^6+2^6+2^6+2^6) = 256\ IL$	$768L$
Modified FGB detector (M2)	$I \times L(2^4+2^4+2^4+2^4) = 64IL$	$192L$

where I is the number of iterations, L is the number of total bits in each block.

Thereby, we can rewrite as

$$M(C;A) = 1 - E\left\{\log_2\left(1+\exp^{-C}\right)\right\} \qquad (35)$$

where A is a measure of uncertainty of the random variable, $E\{.\}$ is the expectation operator.

We show the comparison of the required SNR from 8 to 26 dB of the mutual information for the three detectors: the conventional FGB detector, the modified FGB detector (M1) and the modified FGB detector (M2). The performance of the modified FGB detector (M2) is better than the other detectors on the BPMR channel at areal densities of 2.5 and 3 Tb/in^2, as shown in Fig. 19.

Finally, Table 1 [24] shows the comparisons for the computing complexity of each detector. Considering the complexity of the factor graph on the 2-D interference channel, the factor node is connected to the bit node for each message per edge. The conventional FGB detector has one channel that operates on 2^9 = 512 edges, the modified FGB detector (M1) has 4 channels that operate on 4×2^6 = 256 edges, and the modified FGB detector (M2) has 4 channels that operate on 4×2^4 = 64 edges. Then, the total number of edges between the factor node and the bit node is 1,536, 768, and 192 edges after three iterations, respectively.

5. CONCLUSION

In this paper, we propose two methods to improve the performance of the FGB detectors on the BPMR channel at an areal density of 2.5 and 3 Tb/in^2. Both methods propose separating the coefficients of the 2-D interference channel into four clusters. The first method has six nodes per cluster. The second method has four nodes per cluster. Then, we consider the hierarchical relationship of the channels on the factor graph among the main bit and its neighboring bits. Simulation results show that both modified FGB detectors give better BER performance than the conventional FGB detector. In addition, the modified FGB detectors (M1) and (M2) have less complexity than the conventional FGB detector.

ACKNOWLEDGEMENT

This work was supported in by Department of Electronics Engineering, Faculty of Engineering and Technology, Rajamangala University of Technology Isan, Nakhon Ratchasima, Thailand.

REFERENCES

[1] R. L. White, R. M. H. New, and R. F. W. Pease, "Patterned Media: A Viable Route to 50 Gbit/in^2 and Up for Magnetic Recording?," *IEEE Transactions on Magnetics*, vol. 33, no. 1, pp. 990-995, Jan. 1997.

[2] G. F. Hughes, "Read Channels for Patterned Media," *IEEE Transactions on Magnetics*, vol. 35, no. 5, pp. 2310-2312, Sep. 1999.

[3] Z. Jin, N. Bertram, B. Wilson, and R. Wood, "Simulation of the Off-Track Capability of a One Terabit per Square Inch Recording System," *IEEE Transactions on Magnetics*, vol. 38, no. 2, pp. 1429-1435, Mar. 2002.

[4] P. W. Nutter, I. T. Ntokas, and B. K. Middleton, "An Investigation of the Effects of Media Characteristics on Read Channel Performance for Patterned Media Storage," *IEEE Transactions on Magnetics*, vol. 41, no. 11, pp. 4327-4334, Nov. 2005.

[5] S. Nabavi, S. Jeon, and B. V. K. Vijaya Kumar, "An Analytical Approach for Performance Evaluation of Bit-Patterned Media Channels," *IEEE Journal on Selected Areas in Communications*, vol. 28, no. 2, pp. 135-142, Feb. 2010.

[6] S. Nabavi, B. V. K. Vijaya Kumar, J. A. Bain, C. Hogg, and S. A. Majetich, "Application of Image Processing to Characterize Patterning Noise in Self-Assembled Nano-Masks for Bit-Patterned Media," *IEEE Transactions on Magnetics*, vol. 45, no. 10, pp. 3523-3526, Oct. 2009.

[7] Y. Wang and B. V. K. Vijaya Kumar, "Improved Multitrack Detection With Hybrid 2-D Equalizer and Modified Viterbi Detector," *IEEE Transactions on Magnetics*, vol. 53, no. 10, ID. 3000710, Oct. 2017.

[8] T. A. Nguyen and J. Lee, "Parallel Detection Based on a Generalized Partial Response Target for Staggered Bit-Patterned Media Recording Systems," *IEEE Access*, vol. 10, pp. 62556-62564, Jun. 2022.

[9] B. Fan, P. H. Siegel, and H. K. Thapar, "Generalized Weighted Sum Subtract Joint Detection for a Class of Multihead Multitrack Channels," *IEEE Transactions on Magnetics*, vol. 55, no. 2, ID. 3300111, Feb. 2019.

[10] S. Han, G. Kong, and S. Choi, "A Detection Scheme With TMR Estimation Based on Multi-Layer Perceptrons for Bit Patterned Media Recording," *IEEE Transactions on Magnetics*, vol. 55, no. 7, ID. 3100704, Jul. 2019.

[11] Y. Wang, B. V. K. Vijaya Kumar, Y. Wen, and P. Li, "Channel Modeling and Multi-Island Recording Scheme on Bit-Patterned Media With Long-Range Island Orientation Fluctuations," *IEEE Transactions on Magnetics*, vol. 54, no. 11, ID. 3001407, Nov. 2018.

[12] F. Ghanami and G. A. Hodtani, "Information Theoretical Analysis of a New Write Channel Model for

Bit-Patterned Media Recording," *IEEE Transactions on Magnetics*, vol. 56, no. 4, ID. 3100109, Apr. 2020.

[13] S. Jeong and J. Lee, "Bit-Flipping Scheme Using K-Means Algorithm for Bit-Patterned Media Recording," *IEEE Transactions on Magnetics*, vol. 58, no. 8, ID. 3101704, Aug. 2022.

[14] Y. Qin and J. G. Zhu, "Deep Neural Network: Data Detection Channel for Hard Disk Drives by Learning," *IEEE Transactions on Magnetics*, vol. 56, no. 2, ID. 6701108, Feb. 2020.

[15] M. Nishikawa, Y. Nakamura, Y. Kanai, H. Osawa, and Y. Okamoto, "Improvement of Iterative Decoding With LLR Modulator by Neural Network Using Magnetic Transition Information in SMR System," *IEEE Transactions on Magnetics*, vol. 57, no. 2, ID. 3100105, Feb. 2021.

[16] A. Aboutaled and N. Nangare, "Reduced Complexity Neural Network Equalizers for Two-Dimensional Magnetic Recording," *IEEE Transactions on Magnetics*, vol. 59, no. 3, ID. 3000708, Mar. 2023.

[17] J. Hu, T. M. Duman, M. F. Erden, "Graph-Based Channel Detection for Multitrack Recording Channels," *EURASIP Journal on Advances in Signal Processing*, doi: 10.1155/2008/738281, ID. 738281, pp. 1-9, Nov. 2008.

[18] T. Sopon, P. Supnithi, and K. Vichienchom, "Improved 2-D Graph-Based Detectors for 2-D Interference Channels," *IEEE Transactions on Magnetics*, vol. 50, no. 11, ID. 3101704, Nov. 2014.

[19] J. Moon, and W. Zeng, "Equalization for Maximum Likelihood Detectors," *IEEE Transactions on Magnetics*, vol. 31, no. 2, pp. 1083-1088, Mar. 1995.

[20] S. Nabavi, and B. V. K. Vijaya Kumar, "Two-Dimensional Generalized Partial Response Equalizer for Bit-Patterned Media," *in Proceedings of 2007 IEEE International Conference on Communications (ICC 2007)*, Glasgow, Scotland, pp. 6249–6254, 2007.

[21] T. Sopon, P. Supnithi, and K, Vichienchom, "Performance of Log-MAP Algorithm for Graph-Based Detections on The 2-D Interference Channel," *in Proceeding of The 14th Joint International Conference on Information and Communication Technology, Electronic and Electrical Engineering (JICTEE-2014)*, Chiang Rai, Thailand, 2014.

[22] J. S. Yedidia, W. T. Freeman, and Y. Weiss, "Constructing Free-Energy Approximations and Generalized Belief Propagation Algorithms," *IEEE Transactions on Information Theory*, vol. 51, no. 7, pp. 2282-2312, Jul. 2005.

[23] J. Hagenauer, "The EXIT Chart-Introduction to Extrinsic Information Transfer in Iterative Processing," *in Proceedings of 2004 12th European Signal Processing Conference*, Vienna, Austria, pp. 1541-1548, 2004.

[24] B. Kurkoski, "Towards efficient detection of two-dimensional intersymbol interference channels," *IEICE Transactions on Fundamentals*, vol. E91, no. 10, pp. 2696-2703, Oct. 2008.

Thanomsak Sopon received the B.Eng.degree in Electronics Engineering from Sripatum University, Bangkok, Thailand, in 1998, the M.Eng. degree in Computer Engineering from Khon Kaen University, Khon Kaen, Thailand, in 2010, and the Ph.D. degree in Data Storage Technology from the King Mongkut's Institute of Technology Ladkrabang, Bangkok, Thailand, in 2014. In 2017, he has been an Assistant Professor at Department of Electronics Engineering, Faculty of Engineering and Technology, Rajamangala University of Technology Isan, Nakhon Ratchasima, Thailand. His research interests include data storage technology, digital communications, digital signal processing, and artificial intelligence.